Annals of Botany **126**: 25–37, 2020
doi: 10.1093/aob/mcaa041, available online at www.academic.oup.com/aob

ANNALS OF BOTANY
Founded 1887

Biochemical and mesophyll diffusional limits to photosynthesis are determined by prey and root nutrient uptake in the carnivorous pitcher plant *Nepenthes* × *ventrata*

Sebastià Capó-Bauçà[1], Marcel Font-Carrascosa[1], Miquel Ribas-Carbó[1], Andrej Pavlovič[2] and Jeroni Galmés[1,*]

[1]*Research Group on Plant Biology under Mediterranean Conditions, Universitat de les Illes Balears–INAGEA, Palma, Balearic Islands, Spain and* [2]*Department of Biophysics, Centre of Region Haná for Biotechnological and Agricultural Research, Faculty of Science, Palacký University in Olomouc, Šlechtitelů 27, CZ-78371, Czech Republic*
**For correspondence. E-mail jeroni.galmes@uib.cat*

Received: 2 May 2019 Returned for revision: 20 December 2020 Editorial decision: 9 March 2020 Accepted: 10 March 2020
Electronically published: 16 March 2020

• **Background and Aims** Carnivorous plants can enhance photosynthetic efficiency in response to prey nutrient uptake, but the underlying mechanisms of increased photosynthesis are largely unknown. Here we investigated photosynthesis in the pitcher plant *Nepenthes* × *ventrata* in response to different prey-derived and root mineral nutrition to reveal photosynthetic constrains.
• **Methods** Nutrient-stressed plants were irrigated with full inorganic solution or fed with four different insects: wasps, ants, beetles or flies. Full dissection of photosynthetic traits was achieved by means of gas exchange, chlorophyll fluorescence and immunodetection of photosynthesis-related proteins. Leaf biochemical and anatomical parameters together with mineral composition, nitrogen and carbon isotopic discrimination of leaves and insects were also analysed.
• **Key Results** Mesophyll diffusion was the major photosynthetic limitation for nutrient-stressed *Nepenthes* × *ventrata*, while biochemistry was the major photosynthetic limitation after nutrient application. The better nutrient status of insect-fed and root-fertilized treatments increased chlorophyll, pigment–protein complexes and Rubisco content. As a result, both photochemical and carboxylation potential were enhanced, increasing carbon assimilation. Different nutrient application affected growth, and root-fertilized treatment led to the investment of more biomass in leaves instead of pitchers.
• **Conclusions** The study resolved a 35-year-old hypothesis that carnivorous plants increase photosynthetic assimilation via the investment of prey-derived nitrogen in the photosynthetic apparatus. The equilibrium between biochemical and mesophyll limitations of photosynthesis is strongly affected by the nutrient treatment.

Key words: Carnivorous, CO_2 assimilation, mesophyll conductance, mineral nutrition, *Nepenthes*, nutrient stress, photosynthesis, Rubisco.

INTRODUCTION

Carnivorous plants represent a fascinating example of adaptation to specific environments through the development of effective traits to sustain growth and survivorship. They are adapted to live in nutrient-poor environments because of their ability to obtain nutrients by prey attraction, capture and digestion. This adaptation has been documented in >800 species worldwide, mostly angiosperms (Ellison and Adamec, 2018). Among these, carnivorous plants of the genus *Nepenthes*, with characteristic passive traps called pitchers, have attracted attention to serve as a model plant to study the physiology of carnivorous plants.

In natural habitats, carnivorous plants can capture and digest a wide range of insect prey (Ellison and Gotelli, 2009; Sui and Clarke, 2015). For instance, in *Nepenthes*, ants are the dominant prey type (family Formicidae) but Hymenoptera, Coleoptera and Diptera are also frequent in their diet (Chin *et al.*, 2014). However, these studies have been centred on the description of prey diversity found in traps, while the consequences of different prey-based nutrition on the physiology of the carnivorous plants have not been evaluated, because prey feeding studies are typically assessed with only one type of insect (e.g. Méndez and Karlsson, 1999; Wakefield *et al.*, 2005; Kruse *et al.*, 2014).

Benefits to prey feeding has been attributed to more nitrogen (N) availability (Ellison, 2006). In *Nepenthes*, about 50–71 % of their N may come originally from insect digestion (Schulze *et al.*, 1997; Moran *et al.*, 2001). Nevertheless, other macronutrients such as phosphorus (P), potassium (K) and magnesium (Mg) can also be limiting for carnivorous plants and may also be absorbed from prey (Adamec, 2002; Pavlovič *et al.*, 2014). The cost–benefit model of carnivory proposed by Givnish *et al.* (1984) and subsequent studies (for a review, see Pavlovič and Saganová, 2015) attributed the primary benefit of enhanced nutrient availability to an increment of the photosynthetic capacity, providing more photoassimilates to fuel growth and reproduction of fed plants. Despite some initial discrepancies (Méndez and Karlsson, 1999; Wakefield *et al.*, 2005), subsequent studies

confirmed an increment in the net CO_2 assimilation rate (A_n) after insect feeding in *Sarracenia* (Farnsworth and Ellison, 2008), *Aldrovanda vesiculosa* (Adamec, 2008), *Dionaea muscipula* (Kruse *et al.*, 2014), *Drosera capensis* (Pavlovič *et al.*, 2014) and *Nepenthes* (Pavlovič *et al.*, 2009, 2011; He and Zain, 2012).

In *Nepenthes*, prey feeding increases plant N concentration (Pavlovič *et al.*, 2009; He and Zain, 2012) which was related to higher chlorophyll concentration, enhancement of the maximum quantum efficiency of of photosystem II (PSII; F_v/F_m), the quantum efficiency of PSII (Φ_{PSII}) and the apparent quantum efficiency of CO_2 fixation (Φ_{CO2}) (Pavlovič *et al.*, 2009). Moreover, a higher total soluble protein concentration was found in prey-fed plants (He and Zain, 2012). While convincing evidence is still lacking, it has been suggested that these results were presumably related to higher Rubisco concentration, resulting in higher CO_2 assimilation in fed plants (He and Zain, 2012; Pavlovič and Saganová, 2015). Originally, this was suggested in the cost–benefit model for evolution of botanical carnivory 35 years ago without any experimental evidence (Givnish *et al.*, 1984). The improvement in photosynthesis after prey feeding suggests that biochemistry is the prime determinant for the low rates of CO_2 assimilation typically observed in terrestrial carnivorous plants. However, the photosynthetic CO_2 assimilation may also be constrained because of a constitutive poor capacity to transfer CO_2 towards the chloroplast stroma. In this sense, low stomatal density and a compact leaf mesophyll without a palisade layer have been observed in traps of *Drosera* (Juniper *et al.*, 1989; Méndez and Karlsson, 1999), *Dionaea* (Hodick and Sievers, 1989) and *Nepenthes* pitchers (Pavlovič *et al.*, 2007). In contrast, mesophyll density and stomatal density in *Nepenthes* leaf lamina were comparable with those of non-carnivorous plants (Pavlovič *et al.*, 2007). Since no data are available in the literature on the capacity of the leaf mesophyll to transport CO_2 in carnivorous plants, the actual limitations to photosynthesis are still an unresolved matter in this group of plants.

Accurate estimation of the leaf mesophyll conductance to CO_2 (g_m) requires precise information on several variables included in the mechanistic models of leaf photosynthesis (Farquhar *et al.*, 1980; von Caemmerer, 2000). Among them, the catalytic traits of Rubisco, which differ among plant species (Galmés *et al.*, 2014), are critical inputs of the photosynthetic model (Martins *et al.*, 2013; Perdomo *et al.*, 2016). So far, Rubisco catalytic traits have barely been characterized in carnivorous plants. Galmés *et al.* (2014) showed that Rubisco in carnivorous *Drosera* and *Sarracenia* tends to display a higher intrinsic maximum carboxylation rate (k_{cat}^c) and carboxylation catalytic efficiency (k_{cat}^c/K_c) as compared with other plant groups. However, a full description of Rubisco catalytic traits including the oxygenase parameters is lacking for carnivorous plants.

The aim of the present study was to evaluate the impact of different prey types and soil mineral fertilization on the photosynthetic performance of *Nepenthes* × *ventrata*, a natural hybrid between *Nepenthes ventricosa* Blanco and *Nepenthes alata* Blanco found in the northern forests of the Philippines. In particular, we aimed to describe, for the first time, the main intrinsic limitations of photosynthesis in carnivorous plants and the response to different prey-derived and root mineral nutrition. To assess this, nutrient-stressed plants were fed with four different insect types known to be part of the diet of *Nepenthes* in its natural habitat, and also supplemented with full inorganic solution in the soil. The hypothesis is that different types of nutrition, either by plants fed on different insects or by soil fertilization by mineral solution, can have different implications for CO_2 assimilation capacity, acting at the photochemical, biochemical and biophysical levels.

MATERIALS AND METHODS

Plant material and experimental conditions

Plants were obtained from FleuraMetz (Aalsmeer, The Netherlands) and cultivated in 1 L pots with a soil mixture of *Sphagnum*/perlite/peat. Plants were grown in a chamber with day:night temperatures of 26 °C:18 °C and 50–70 % relative air humidity. During experiments, photosynthetically photon flux density (PPFD) at the canopy level was 200 µmol m^{-2} s^{-1} with a 12 h:12 h light:dark photoperiod.

After receiving the plants from the nursery, they were subjected to nutritional stress by thoroughly watering the pots with distilled water once every 2 d. To prevent entry of prey into pitchers, they were plugged with wads of cotton wool moistened in distilled water. This procedure was maintained over 18 weeks during which plants gradually expressed signs of nutritional stress such as reduced chlorophyll concentration and growth reduction (Supplementary data Fig. S1). Before treatment application, all plants were at the same age and height, and had a similar number of leaves and pitchers.

After these 18 weeks of nutritional stress, a group of four plants were analysed (group *C0*) as detailed below. Then, six different treatments were applied on four plants per treatment. In treatment *C*, distilled water was applied to the soil once every 2 d to continue with the nutritional stress conditions. In treatment *I*, 3.125 mL of adjusted inorganic solution diluted in distilled water was administered to the soil once per week. The final concentration of inorganic solution in this treatment was 12.0 mM KNO_3, 180.26 mM $Ca(NO_3)_2{\cdot}4H_2O$, 22.0 mM NaH_2PO_4 and 2.63 mM $MgSO_4{\cdot}7H_2O$, and micronutrients were adjusted with Hoagland's solution (Shi *et al.*, 2016).

In the remaining four treatments, prey-derived nutrition was performed by feeding plants with 0.3 g per week of different insects: wasps (treatment *W*), ants (treatment *A*), beetles (treatment *B*) and flies (treatment *F*). Insects were dropped in different newly opened pitchers coinciding with administration of inorganic solution in treatment *I*. In order to avoid water stress, all plants were watered with distilled water once every 2 d. All treatments were maintained for 9 weeks, after which plants were measured as explained below. All measurements were performed on four individual plants and on fully expanded leaves which emerged during treatment application.

Insects were obtained from natural environments: *Polistes fuscatus* (wasps, *W*) and *Musca domestica* (flies, *F*) from Son Suau (Manacor, Balearic Islands), *Crematogaster scutellaris* (ants, *A*) from Son Macià (Manacor, Balearic Islands) and *Phyllognathus silenus* (beetles, *B*) from Cala Morlanda (Manacor, Balearic Islands). Immediately after capture, insects were frozen and stored at –20 °C. The insect-fed and root-fertilized treatments were adjusted to provide a similar amount of N, P and K to the plants.

Plant growth and biomass allocation to fractions

The total numbers of leaves and pitchers per plant were counted, as well as those which emerged during the period of treatment application. Necrotic pitchers were attributed to those where necrotic tissue affected all the peristome, while pitchers in formation were the closed pitchers.

Total plant leaf area was measured using ImageJ (Wayne Rasband National Institutes of Health, USA) in detached leaves. The increment of leaf area during the period of treatment application was obtained by subtracting the leaf area of group *C0*.

At the end of the treatment application period, all plant tissues were collected and divided into four fractions: pitchers, leaves, stems and roots. The dry weight was obtained by weighting dried fractions at 70 °C for 72 h in an oven. The increment in total and fraction biomass was calculated by subtracting the biomass of group *C0*.

Gas exchange and chlorophyll a *fluorescence measurement*

Gas exchange and chlorophyll *a* fluorescence were analysed with an open infrared gas exchange analyser system equipped with a leaf chamber fluorometer (Li-6400-40, Li-Cor Inc., Lincoln, NE, USA). Measurements were performed on fully expanded leaves which emerged during treatment application at a leaf temperature of 25 °C and a gas flow of 150 µmol mol^{-1}.

After inducing steady-state photosynthesis for at least 30 min at an ambient CO_2 concentration (C_a) of 400 µmol mol^{-1}, photosynthesis responses to varying substomatal CO_2 concentrations (A_n–C_i) were measured as explained in Galmés *et al.* (2007) and consisted of 12 measurements per curve. Four A_n–C_i curves were performed per treatment on different individuals. Light conditions in the leaf chamber were 1700 µmol m^{-2} s^{-1} of PPFD with 10 % blue light. Corrections for the CO_2 leakage in and out of the leaf chamber of the Li-6400 were applied to all gas exchange data, as described by Flexas *et al.* (2007).

Simultaneous measurements of chlorophyll *a* fluorescence were made at each C_a of the A_n–C_i curve. The quantum efficiency of PSII (Φ_{PSII}) was determined as:

$$\Phi_{PSII} = (F'_m - F_s)/F'_m \quad (1)$$

where F_s is the steady-state fluorescence in the light (PPFD 1700 µmol quanta m^{-2} s^{-1}) and F'_m the maximum fluorescence obtained with a light-saturating pulse (8500 µmol quanta m^{-2} s^{-1}). Since Φ_{PSII} represents the quantum yield of PSII, the rate of electron transport (J) was calculated using the equation:

$$J = \Phi_{PSII} \times PPFD \times \alpha \times \beta \quad (2)$$

where α is the leaf absorbance and β is the distribution of absorbed energy between the two photosystems. The product $\alpha \times \beta$ was determined as explained by Martins *et al.* (2013) with the relationship between Φ_{PSII} and Φ_{CO2} obtained by varying C_a under non-photorespiratory conditions in a nitrogen atmosphere containing less than 2% (v/v) O_2.

From measurements of gas exchange and chlorophyll *a* fluorescence, mesophyll conductance to CO_2 (g_m) was estimated at each C_i according to Harley *et al.* (1992) using the equation:

$$g_m = A_n / < C_i - \{\Gamma^* [J + 8(A_n + R_l)]\} / [J - 4(A_n + R_l)] > \quad (3)$$

Half of the mitochondrial respiration rate in darkness (R_{dark}), measured as indicated below, was used as a proxy for the rate of mitochondrial respiration in the light (R_l). The chloroplast CO_2 compensation point (Γ^{*vitro}) was calculated from the *in vitro* specificity factor of Rubisco ($S_{c/o}$) at 25 °C determined as explained in Supplementary data Method S1:

$$\Gamma^{*vitro} = 0.5 O_A / S_{c/o}{}^{vitro} \quad (4)$$

A_n–C_i curves were transformed into A_n vs. chloroplastic CO_2 concentration (C_c) curves converting each C_i to C_c using the estimated values of g_m. From A_n–C_c curves, the maximum velocity of carboxylation *in vivo* ($V_{cmax}{}^{in\ vivo}$) and the maximum capacity for electron transport rate (J_{max}) were calculated as in Bernacchi *et al.* (2001). Considering that Rubisco kinetic properties can vary among plant species and its implication in modelling photosynthetic response (Hermida-Carrera *et al.*, 2016), the Farquhar *et al.* (1980) model was fitted using the specific kinetic parameters of Rubisco determined *in vitro* for *Nepenthes* × *ventrata* (see below and Supplementary data Method S1).

The photosynthesis response to varying PPFD conditions was measured by changing the PPFD of the leaf chamber from 0 to 1700 µmol photons m^{-2} s^{-1}. Four A_n–PPFD curves were performed per treatment on different plant individuals at a C_a of 400 µmol mol^{-1}. Simultaneous measurements of chlorophyll *a* fluorescence were made at each PPFD of the A_n–PPFD curve. The apparent quantum yield of CO_2 fixation (Φ_{CO2}) was determined as the slope of the light response curve between 0 and 200 µmol m^{-2} s^{-1} PPFD (Farquhar *et al.*, 1980). The quantum efficiency of PSII (Φ_{PSII}) was determined using eqn (1).

Dark measurements

The dark respiration rate (R_{dark}) and the maximum quantum efficiency of PSII (F_v/F_m) were measured at pre-dawn using the Li-6400-40. Conditions in the leaf cuvette were: gas flow at 150 µmol s^{-1}, C_a of 400 µmol mol^{-1} and leaf temperature of 25 °C. A measuring light of 0.5 µmol photon m^{-2} s^{-1} was set at a frequency of 600 Hz to determine the zero fluorescence level (F_o). To achieve the maximum fluorescence level (F_m), saturation pulses of 8500 µmol photon m^{-2} s^{-1} for 0.8 s were applied. Dark measurements of gas exchange and chlorophyll *a* fluorescence consisted of four replicates per treatment on different individuals.

Analysis of photosynthetic limitations

The quantitative limitation analysis of photosynthetic CO_2 assimilation was calculated for each plant as in Galmés *et al.* (2017). Stomatal (l_s), leaf mesophyll (l_{mc}) and biochemical (l_{bc}) limitations were calculated as:

$$l_s = \frac{\frac{g_{tot}}{g_s} \times \frac{A_n}{C_c}}{g_{tot} + \frac{A_n}{C_c}} \quad (5)$$

$$l_{mc} = \frac{\frac{g_{tot}}{g_m} \times \frac{A_n}{C_c}}{g_{tot} + \frac{A_n}{C_c}} \quad (6)$$

$$l_{bc} = \frac{g_{tot}}{g_{tot} + \frac{A_n}{C_c}} \quad (7)$$

The total leaf conductance to CO_2 (g_{tot}) was obtained as the sum of mesophyll and stomatal conductance to CO_2 considering that both are in series ($1/g_{tot} = 1/g_s + 1/g_m$).

Rubisco kinetic parameters

Rubisco kinetic measurements were performed on crude extracts obtained by grinding approx. 0.4 g of leaves (fresh weight) as explained in Supplementary data Method S1.

Leaf anatomical measurements

On each plant, leaf mass area (LMA) was determined by subtracting six cores of leaf lamina (0.78 cm^2 each core) and calculating their dry weight:area ratio. The leaf mesophyll anatomy was inspected to assess the fraction of the mesophyll occupied by intercellular air spaces (f_{ias}) and cell wall thickness (T_{cw}). For this, 1 × 1 mm pieces were cut off between the main veins of the leaves for anatomical measurements. Semi-fine (0.8 µm) and ultra-fine (90 nm) cross-sections were obtained as described by Carriquí *et al.* (2015) for each plant using both optical and transmission electron microscopy. All images were analysed using ImageJ (Wayne Rasband National Institutes of Health, USA).

Chlorophyll, total soluble protein and Rubisco concentration in leaves

Leaf samples of 0.2 g of fresh weight per plant were rapidly frozen in liquid nitrogen. Each sample was ground to fine powder in liquid N and homogenized in 1 mL of extraction buffer [100 mM Bicine pH 8.0, 1 mM EDTA, 5 mM MgCl and 5 mM dithiothreitol (DTT)], 2 % polyethyleneglycol (PEG) 4000 and 10 µL of protein inhibitor cocktail (P9599, Sigma-Aldrich, USA). The homogenate was centrifuged at 13 000 rpm for 4 min at 4 °C. The supernatant was utilized to determine total soluble protein (TSP) following Bradford (1976) and photosynthetic pigments as in Lichtenthaler and Wellburn (1983).

Two aliquots (100 µL each) of the same supernatant were used to quantify the concentration of Rubisco catalytic sites and its activation state by [^{14}C]CABP (2-C-carboxy-D-arabinitol 1,5-bisphosphate) binding sites (Kubien *et al.*, 2011). One of these aliquots was previously activated with 100 µL of activation buffer (50 mM EPPS-NaOH at pH 8.0, 1 mM EDTA, 20 mM $NaHCO_3$ and 20 mM $MgCl_2$). Rubisco activation was calculated as the percentage of total catalytic sites with respect to catalytic sites in fully activated Rubisco.

Western blot analysis

Western blot analysis was done in protein extracts of 100 mg of *Nepenthes* lamina as detailed in Supplementary data Method S2.

Mineral composition of insects and leaves

Just before harvesting plants for biomass measurements, two mixed samples for each insect species were made. One of the mixed samples was made with digested insect carcasses taken from the pitchers of fed plants, and the other was made with intact insects. In addition, leaf lamina samples of 2.5 g f. wt, without including midribs or tendrils, were taken from each plant. All samples were dried at 70 °C for 72 h in an oven. After grinding to a fine powder, Al, B, Ca, Cd, Co, Cu, Fe, K, Mg, Mn, Na, Ni, P, Pb, Rb, S, Sr, Ti and Zn were analysed by element inductively coupled plasma optical emission spectrometry (iCAP 6500-ICP-OES Spectrometer ICP-OES, Thermo Scientific, USA). Total carbon and nitrogen concentration were also analysed using an Elemental Analyzer (TRUSPEC, LECO Corporation, USA).

The percentage of element removed by digestion was calculated as in Dixon *et al.* (1980) using the difference between digested and non-digested insects using the following equation:

$$\text{Digestion}(\%) = \frac{\begin{array}{l}\text{Quantity of element}\\ \text{in insect before}\\ \text{digestion (mg or } \mu\text{g)}\end{array} - \begin{array}{l}\text{Quantity of element}\\ \text{in insect after}\\ \text{digestion (mg or } \mu\text{g)}\end{array}}{\begin{array}{l}\text{Quantity of element}\\ \text{in insect before}\\ \text{digestion (mg or } \mu\text{g)}\end{array}} \times 100$$

Carbon and nitrogen isotopic discrimination of insects and leaves

Carbon and nitrogen isotopic composition were determined in the same samples used for the mineral composition of the insects and the leaves. Carbon and nitrogen isotopic composition were also measured in soil samples taken from insect-fed treatments. These samples were washed with distilled water to remove possible mineral nutrients and then dried at 70 °C for 72 h before being ground. Also, a sample of the mixture of chemical reagents utilized for the inorganic solution was taken to determine the C and N isotopic composition of the inorganic solution.

All samples were combusted in an elemental analyser (Thermo Flash EA 1112 Series, Bremen, Germany), and CO_2 and N_2 were directly injected into a continuous-flow isotope ratio mass spectrometer (Thermo-Finnigan Delta XP, Bremen, Germany) for isotope analysis. Peach leaf standards (NIST 1547) were run every six samples. The standard deviation of the analysis was <0.1 ‰. Results are presented as δ vs. PDB (Pee Dee Belemnite) for C and as δ vs. atmospheric N_2 air for N.

The percentage of leaf N derived from the insects was calculated as in Schulze *et al.* (1991) using the following equation:

$$\begin{array}{l}\text{Leaf N derived from}\\ \text{insects(\%)}\end{array} = \frac{\delta^{15}N_p - \delta^{15}N_r}{\delta^{15}N_i - \delta^{15}N_r} \times 100 \quad (8)$$

where $\delta^{15}N_p$ was $\delta^{15}N$ of the treated plant, $\delta^{15}N_r$ was $\delta^{15}N$ of the reference ($\delta^{15}N$ initial group, *C0*) and $\delta^{15}N_i$ was $\delta^{15}N$ of the insect.

Statistical analysis

The Anderson–Darling test and Bartlett test were carried out to test normality and variance homogeneity, respectively. Differences between treatments were assessed using one-way analysis of variance (ANOVA). To find differences between means, Duncan's

test was used. Student's *t*-test was performed to find differences in Rubisco kinetic parameters between *Nepenthes* × *ventrata* and *Triticum aestivum*. Correlation coefficients and significance were determined on direct data (n = 18–28, depending on the correlation) and using the Pearson method. *P*-values <0.05 were considered significant. Data were analysed using R (version 3.2.3, 2015-12-10) with Rstudio interphase (RStudio Version 0.99.879© 2009–2016, Inc.) and plotted using the ggPlot2 package (ggPlot2 version 2.2.1; Springer-Verlag, New York, 2009–2016).

RESULTS

The effect of insect feeding and root fertilization on the leaf mineral composition

Insect-fed and root-fertilized treatments increased leaf N concentration as compared with treatment *C* and group *C*0. In contrast, other macronutrients such as K, P and Na were generally more concentrated in treatment *C* (Table 1; Supplementary data Table S1). Notably, these differences were mitigated when total leaf tissue was taken into account (Supplementary data Table S2), indicating dilution of K, P and Na in the new leaf tissue due to the more intensive stimulated growth of treated plants.

The isotopic discrimination of N showed a significant correlation between insect and plant δ^{15}N (Fig. 1), suggesting that the major N source of insect-fed treatments was N from insects and not from root uptake. The percentage of plant N derived from the insect was lower in treatment *A* (Table 2), probably due to a lower digestion and/or availability of N from ants as compared with the other insects (Supplementary data Table S3). Regarding the other macronutrients, their digestion was efficient according to the difference between before and after insect digestion, except in the case of Ca and C (Supplementary data Table S3). Leaf carbon isotopic discrimination was similar between insect-fed and root-fertilized treatments, with less negative δ^{13}C values in treatment *C* and group *C0* (Table 2).

Treatment-induced changes in the leaf mineral composition and altered leaf biochemistry

There was a trend for an increased concentration of leaf TSP, chlorophyll, carotenoids and Rubisco catalytic sites in plants supplied with inorganic solution or fed with insects as compared with treatment *C* and group *C0* (Table 3), although the significant differences among treatments depended on each parameter. For instance, for leaf TSP, differences were only observed between treatments *W* and *C* (and group *C0*), while for Rubisco catalytic sites differences were much more evident when comparing treatment *C* and group *C0* with the other treatments. In any case, changes in the concentration of total chlorophyll, Rubisco and TSP correlated positively with changes in the leaf N concentration among treatments (Fig. 2).

Immunoblotting of photosynthesis-related proteins showed a general accumulation of chlorophyll-binding proteins of PSI and PSII in plants supplied with inorganic solution or fed with insects, corresponding to the higher amount of chlorophyll in these treatments. Moreover, all treatments also increased the relative abundance of components of the oxygen-evolving complex (PsbO, PsbP and PsbQ), electron transport, ATPase and Rubisco (mainly the RbcS subunit). The only protein with a higher relative concentration in treatment *C* was PsbS, involved in non-photochemical quenching (Fig. 3).

Table 1. *Summarized table of Fisher's values* (F) *with the level of significance obtained by ANOVA* (P) *for the comparison among treatments of the mineral concentration of leaves of* Nepenthes × ventrata

Element	*F*	*Pj*
N (mg g^{-1} d. wt)	20.94	***
C (mg g^{-1} d. wt)	2.39	n.s.
Ca (mg g^{-1} d. wt)	7.85	***
K (mg g^{-1} d. wt)	14.72	***
Mg (mg g^{-1} d. wt)	6.93	***
Na (mg g^{-1} d. wt)	6.43	***
P (mg g^{-1} d. wt)	7.56	***
S (mg g^{-1} d. wt)	17.25	***
Al (µg g^{-1} d. wt)	0.20	n.s.
B (µg g^{-1} d. wt)	9.34	***
Cd (µg g^{-1} d. wt)	1.67	n.s.
Co (µg g^{-1} d. wt)	0.63	n.s.
Cu (µg g^{-1} d. wt)	2.58	*
Fe (µg g^{-1} d. wt)	1.00	n.s.
Mn (µg g^{-1} d. wt)	2.43	n.s.
Ni (µg g^{-1} d. wt)	2.87	*
Pb (µg g^{-1} d. wt)	0.85	n.s.
Rb (µg g^{-1} d. wt)	20.50	***
Sr (µg g^{-1} d. wt)	9.17	***
Ti (µg g^{-1} d. wt)	0.68	n.s.
Zn (µg g^{-1} d. wt)	3.91	**

Absolute values are shown in Supplementary data Table S1. n.s., not significant; *P < 0.05; **P < 0.01; ***P < 0.001.

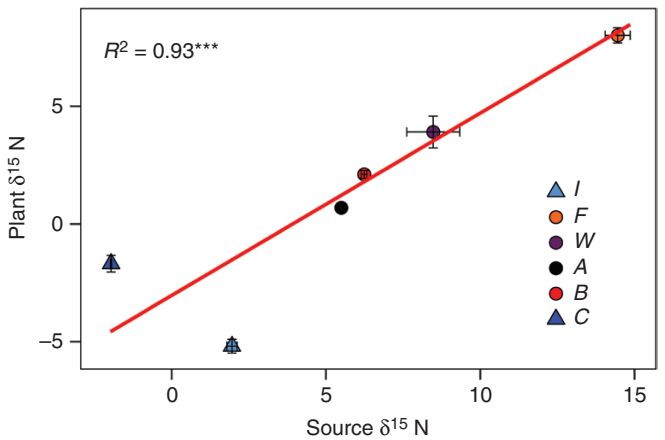

Fig. 1. Correlation between plant δ^{15}N and source δ^{15}N (insect, soil or inorganic solution). Points are the means ± s.e. of different treatments: *C* = control, *B* = beetles, *A* = ants, *W* = wasps, *F* = flies, *I* = root fertilized with inorganic solution. Regression was performed only with insect-fed treatments, represented as points. R^2 is Pearson's regression coefficient, and asterisks show the significance of test correlation (*P < 0.05; **P < 0.01; ***P < 0.001).

The photosynthetic performance of Nepenthes × ventrata *under insect-fed and root-fertilized treatments*

The Rubisco kinetic parameters of *Nepenthes* × *ventrata* determined *in vitro* at 25 °C are listed in Table 4. As compared with wheat, Rubisco from *Nepenthes* × *ventrata* displayed a

Table 2. *Isotopic discrimination of C and N of plants, and the percentage of plant N derived from insect N*

Treatment	$\delta^{13}C$ (‰)	$\delta^{15}N$ (‰)	% of plant N derived from N of insects
I	–31.2 ± 0.1^{c}	–5.20 ± 0.29^{f}	–
F	–31.2 ± 0.1^{c}	8.01 ± 0.32^{a}	54.6 ± 2.2^{ab}
W	–31.4 ± 0.0^{c}	3.90 ± 0.68^{b}	67.1 ± 11.9^{ab}
A	–31.1 ± 0.3^{bc}	0.69 ± 0.16^{d}	10.3 ± 2.8^{c}
B	–31.3 ± 0.1^{c}	2.11 ± 0.17^{c}	32.7 ± 2.8^{bc}
C	–30.6 ± 0.1^{a}	–1.69 ± 0.35^{e}	–
C0	–30.8 ± 0.1^{ab}	0.09 ± 0.27^{d}	–

Values are means ± s.e. Different letters show significant differences in each parameter ($P < 0.05$, post-hoc Duncan's test, $n = 4$).
Treatments are *C0* = initial group, *C* = control, *B* = beetles, *A* = ants, *W* = wasps, *F* = flies, *I* = root fertilized with inorganic solution.

Table 3. *Biochemical data of* Nepenthes × ventrata *leaves*

Parameter	*I*	*F*	*W*	*A*	*B*	*C*	*C0*
TSP (g m^{-2})	2.14 ± 0.20^{ab}	2.22 ± 0.21^{ab}	2.32 ± 0.18^{a}	2.09 ± 0.16^{ab}	2.06 ± 0.17^{ab}	1.74 ± 0.12^{bc}	1.49 ± 0.10^{c}
Chl *a* (mg m^{-2})	143.5 ± 22.4^{ab}	160.2 ± 4.7^{a}	134.2 ± 7.6^{abc}	104.3 ± 6.6^{c}	120.8 ± 6.3^{bc}	72.0 ± 3.7^{d}	42.1 ± 4.3^{e}
Chl *b* (mg m^{-2})	41.5 ± 5.4^{a}	33.4 ± 8.7^{ab}	41.6 ± 3.2^{a}	27.6 ± 7.0^{ab}	36.9 ± 2.3^{a}	19.5 ± 2.3^{bc}	10.4 ± 2.7^{c}
Chl *a* + *b* (mg m^{-2})	185.0 ± 26.8^{a}	193.6 ± 9.9^{a}	175.7 ± 8.6^{a}	131.9 ± 11.7^{b}	157.7 ± 5.3^{ab}	91.5 ± 6.0^{c}	52.5 ± 6.2^{d}
Carotenoids (mg m^{-2})	69.2 ± 12.0^{a}	69.4 ± 6.7^{a}	59.3 ± 6.0^{ab}	44.1 ± 3.9^{bc}	56.4 ± 8.2^{ab}	27.7 ± 2.1^{cd}	19.1 ± 2.6^{d}
Rubisco activation (%)	84.1 ± 2.0^{a}	83.7 ± 4.0^{a}	82.5 ± 3.1^{ab}	68.4 ± 3.1^{c}	77.8 ± 4.2^{abc}	70.3 ± 4.2^{bc}	68.7 ± 6.0^{c}
Rubisco content (μmol sites m^{-2})	2.15 ± 0.19^{ab}	2.00 ± 0.10^{ab}	2.37 ± 0.32^{a}	1.94 ± 0.06^{ab}	1.68 ± 0.15^{b}	0.90 ± 0.04^{c}	0.97 ± 0.16^{c}
[Rubisco]/TSP (%)	7.10 ± 0.91^{a}	6.41 ± 0.84^{ab}	7.00 ± 0.67^{a}	6.54 ± 0.71^{ab}	5.81 ± 0.81^{ab}	3.62 ± 0.35^{c}	4.47 ± 0.76^{bc}

TSP = total soluble protein.
Values are means ± s.e. Different letters show significant differences in each parameter ($P < 0.05$, post-hoc Duncan's test, $n = 4$).
Treatments are *C0* = initial group, *C* = control, *B* = beetles, *A* = ants, *W* = wasps, *F* = flies, *I* = root fertilized with inorganic solution.

similar affinity for CO_2 under atmospheric conditions (K_c^{air}) and maximum rates of oxygenation (k_{cat}^{o}), while presenting a higher affinity for CO_2 under zero oxygen (K_c) and for O_2 (K_o), and a lower maximum rate of carboxylation (k_{cat}^{c}). As a result of these differences, the relative specificity of Rubisco for carboxylation and oxygenation ($S_{c/o}$) was notably lower in *Nepenthes* × *ventrata* in relation to wheat.

The values of net CO_2 assimilation rate (A_n), stomatal conductance (g_s), leaf mesophyll conductance to CO_2 (g_m) and leaf total conductance to CO_2 (g_{tot}) were higher in plants subjected to insect-fed and root-fertilized treatments compared with treatment *C* and group *C0* (Table 5). An exception to this rule was treatment *B*, whose values were non-significantly different from those of treatment *C* and group *C0*. Differences among treatments *I*, *F*, *W* and *A* were minor and restricted to particular cases. A_n was higher in insect-fed and root-fertilized treatments under most chloroplastic CO_2 concentrations (Supplementary data Fig. S2a). There was a trend toward an increased rate of mitochondrial respiration (R_{dark}) in treated plants although only significant for treatments *I* and *A* (Table 5). This is consistent with an increased concentration of cytochrome (COX) and alternative oxidase (AOX) in treated plants in comparison with treatment *C* (Fig. 3).

Both the maximum velocities of Rubisco carboxylation ($V_{cmax}^{in\ vivo}$) and electron transfer (J_{max}) were higher in all insect-fed treatments and the root-fertilized treatment in relation to treatment *C* and group *C0*. Among insect-fed and root-fertilized treatments, the highest values of $V_{cmax}^{in\ vivo}$ and J_{max} were observed in plants fed with ants, while the lowest was seen in plants supplied with the inorganic solution (Table 5). The values of $V_{cmax}^{in\ vivo}$ corresponded to values of $V_{cmax}^{in\ vitro}$ (Fig. 4). Also, $V_{cmax}^{in\ vivo}$ values correlated with Rubisco concentration, but did not correlate with Rubisco activation (Fig. 4). Treatments *F* and *I* displayed higher Rubisco activation as compared with treatments *C* and *A* and group *C0* (Table 3).

In general, photochemistry also improved in insect-fed and root-fertilized plants, with a trend for an increased maximum quantum yield of PSII (F_v/F_m), electron transport rate (J) and apparent quantum yield of CO_2 fixation (Φ_{CO2}) (Table 5). This trend was also manifested in a higher quantum yield of PSII over the whole range of PPFD (Supplementary data Fig. S2b). The tendency in F_v/F_m and J was partly explained by the increase in the total chlorophyll concentration, as indicated by the positive correlation between these parameters (Supplementary data Fig. S3), and by the increase in the amount of chlorophyll-binding proteins and components of the oxygen-evolving complex (Fig. 3).

The observed variation in A_n correlated positively with g_{tot} ($R^2 = 0.94$, $P < 0.001$) and $V_{cmax}^{in\ vivo}$ ($R^2 = 0.48$, $P < 0.001$), suggesting that both leaf CO_2 diffusion and biochemistry played a role in setting the photosynthetic capacity of *Nepenthes* × *ventrata*. A positive relationship was also observed between A_n and g_s ($R^2 = 0.80$, $P < 0.001$), and between A_n and g_m ($R^2 = 0.83$, $P < 0.001$), indicating that both the stomata and mesophyll limited CO_2 diffusion. In the quantitative analysis of photosynthesis (Fig. 5), mesophyll limitation (l_{mc}) was the major constraint for carbon assimilation for nutrient-stressed plants (treatment *C*). In contrast, biochemical limitation (l_{bc}) was the main photosynthetic limitation in all insect-fed and root-fertilized treatments, presenting a higher impact in treatment *I* and group *C0*. Stomatal limitation (l_s) presented higher values in treatment *B* than in treatments *C* and *I* (Fig. 5).

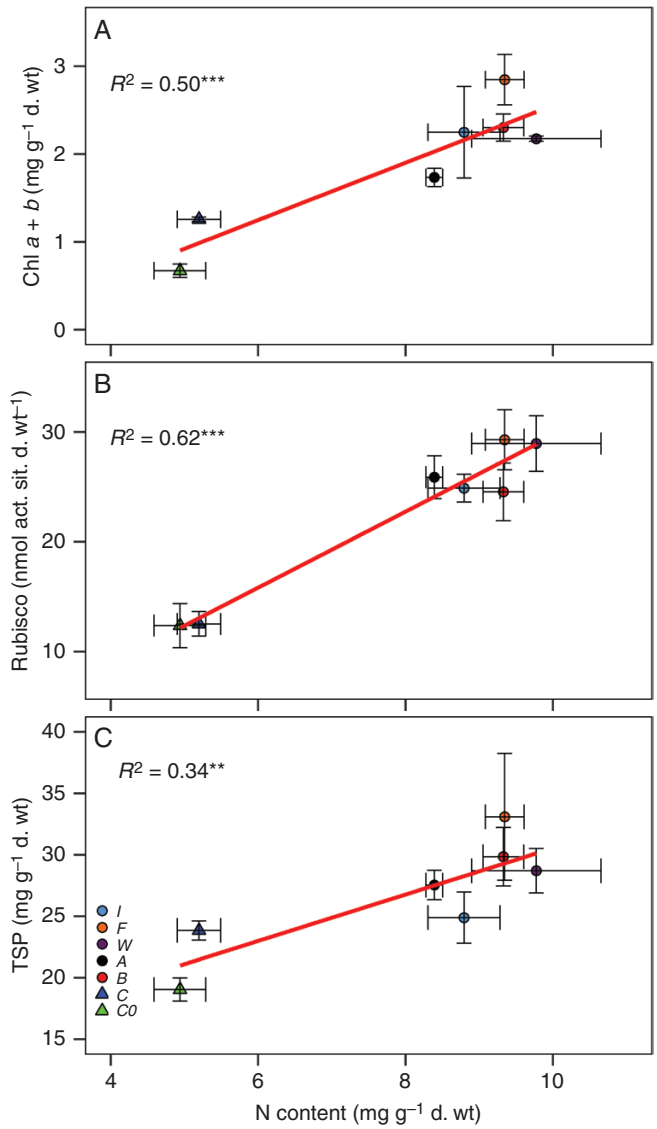

FIG. 2. Correlation between (A) leaf total chlorophyll content and leaf N content; (B) Rubisco catalytic site concentration and leaf N content; (C) leaf total soluble protein (TSP) content and leaf N content. Points are means ± s.e. of different treatments: *C0* = initial group, *C* = control, *B* = beetles, *A* = ants, *W* = wasps, *F* = flies, *I* = root fertilized with inorganic solution. R^2 is Pearson's regression coefficient, and asterisks show the significance of test correlation (*$P < 0.05$; **$P < 0.01$; ***$P < 0.001$).

Leaf anatomical adjustments of Nepenthes × ventrata *in response to treatments*

There were no differences in the LMA among treatments (Table 6; Supplementary data Fig. S4). The fraction of the total mesophyll occupied by intercellular air spaces (f_{ias}) was similar for all treatments, as was the fraction of spongy mesophyll f_{ias}. However, differences were found in the fraction of palisade mesophyll f_{ias} among treatments, with a trend for an increased value in plants under insect-fed and root-fertilized treatments compared with treatment *C* and group *C0* plants (Table 6). A similar response was observed for the cell wall thickness (T_{cw}), with a trend to decrease in the insect-fed and root-fertilized treatments for palisade T_{cw}, and non-significant differences for the overall leaf mesophyll and spongy T_{cw}. A negative correlation was found between palisade T_{cw} and g_m (Fig. 6), suggesting that the changes observed in g_m in response to the different treatments were in part due to adjustments in the anatomy of the leaf palisade cells.

Effect of root-fertilized and insect-fed treatments on growth and biomass allocation

In general, the increase in leaf area and the number of newly developed leaves and pitchers were lower in treatment *C* as compared with the root-fertilized and insect-fed treatments, with the highest values found in treatment *I* (Supplementary data Table S4). The percentage of necrotic pitchers was higher in treatment *C* compared with the other treatments (Supplementary data Table S4). In contrast, treatment *C* showed a lower percentage of pitchers in formation.

Although only treatments *I* and *W* displayed a higher growth rate than treatment *C*, plant growth presented a trend to increase in the insect-fed and the root-fertilized treatments (Supplementary data Table S4). In addition, treatment *I* distributed more sources to leaves than insect-fed and control treatments, which allocated more biomass to pitcher formation (Supplementary data Fig. S5).

DISCUSSION

Both insect-fed and root-fertilized treatments improve the leaf mineral status of nutrient-stressed Nepenthes × ventrata

Both different prey-derived and root mineral nutrition increased the leaf N concentration in nutrient-stressed *Nepenthes* × *ventrata* (Table 1; Supplementary data Table S1), as previously observed in other carnivorous species (Pavlovič *et al.*, 2009, 2010, 2014; He and Zain, 2012; Gao *et al.*, 2015). The proportion of leaf N derived from the insects (Table 2) matched the previous reported range for species of the genus *Nepenthes* (Schulze *et al.*, 1997; Moran *et al.*, 2001; Pavlovič *et al.*, 2011).

The N isotopic discrimination signature confirmed that insect feeding was the main source of leaf N in insect-fed plants (Fig. 1), but differences in N bioavailability among insects were found. Plants fed with ants (treatment *A*) presented lower values of N pitcher digestion (with regard to the difference between nutrient content before and after insect digestion) and leaf N proportion derived from insects (Supplementary data Table S3 and Table 2, respectively). This can be explained by the different bioavailability of insect N which is mainly bound in protein and chitin. Because large quantities of N remain in insect carcasses after digestion in carnivorous plants (Supplementary data Table S3), it has been assumed that part of this N is bound to the insect chitin exoskeleton (Adamec, 2002; Pavlovič *et al.*, 2014). Indeed, carnivorous plants can effectively digest mainly N bound in protein, not chitin (Pavlovič *et al.*, 2016), and insect species strongly differ in chitin (5–20 % of d. wt) and protein content (15–81 % of d. wt; Ramos-Elorduy *et al.*, 1997; Klunder *et al.*, 2012; Kouřimská and Adámková, 2016).

The concentration of the other macronutrients P, K, S, Mg, Ca and Na did not increase in the insect-fed and root-fertilized

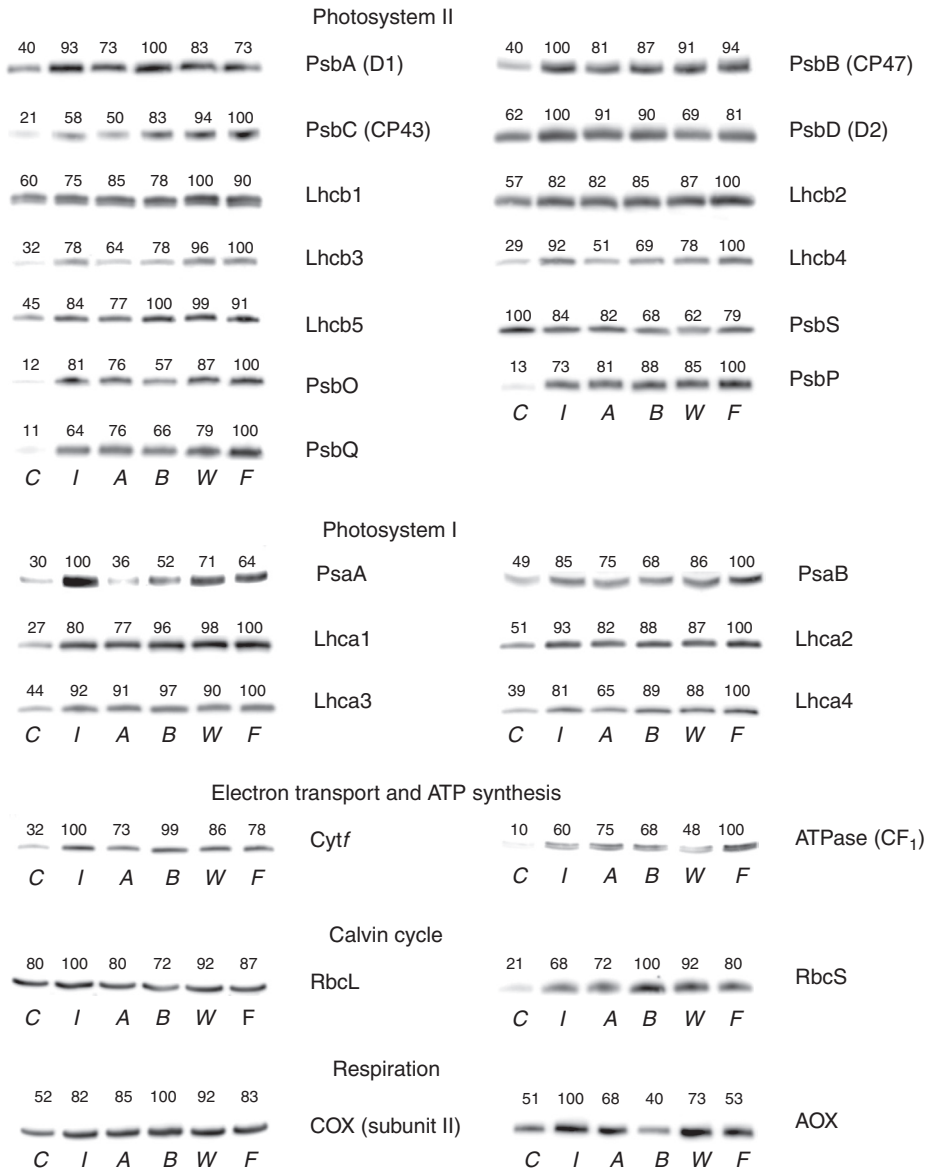

FIG. 3. Immunoblotting of photosynthesis-related proteins in *Nepenthes* × *ventrata* in response to application of inorganic solution or feeding. The same amount of total protein (30 µg) was electrophoresed in a 10% (v/v) SDS–polyacrylamide gel and subjected to western blot analysis. Protein content in the bands was quantified by chemiluminescence. The blots shown are representatives of three independent samples. Treatments are *C* = control, *I* = root fertilized with inorganic solution, *A* = ants, *B* = beetles, *W* = wasps, *F* = flies.

TABLE 4. *Rubisco kinetics of* Nepenthes × ventrata *at 25 °C*

Species	K_c (µM)	K_c^{air} (µM)	k_{cat}^c (s^{-1})	$S_{c/o}$ (mol mol^{-1})	K_o (µM)	k_{cat}^o (s^{-1})
Nepenthes × *ventrata*	7.25 ± 0.28[a]	13.2 ± 0.8[a]	1.44 ± 0.06[a]	59.2 ± 2.5[a]	344.1 ± 52.9[a]	1.14 ± 0.23[a]
Triticum aestivum	8.46 ± 0.43[b]	12.0 ± 1.3[a]	2.23 ± 0.21[b]	97.0 ± 0.6[b]	695.4 ± 169.5[b]	1.90 ± 0.53[a]

Parameters shown are Michaelis–Menten constant for CO_2 at 0% O_2 (K_c), 21% O_2 (K_c^{air}) and for O_2 (K_o); Rubisco CO_2/O_2 specificity ($S_{c/o}$), the maximum carboxylation rate (k_{cat}^c) and maximum oxygenation rate (k_{cat}^o).

Values are means ± s.e. Different letters show significant differences in each parameter ($P < 0.05$, Student's *t*-test, $n = 3$).

treatments and, for some of them, it was even higher in the control treatment (Table 1; Supplementary data Table S1). However, with regard to the mineral composition of the insects before and after feeding, pitcher digestion of these elements was efficient, except in the case of Ca (Supplementary data Table S3). Pavlovič *et al.* (2014) found similar results with K, which was effectively digested from the insect but its concentration decreased in the leaves of fed *Drosera capensis* plants. This fact was attributed to a dilution effect due to enhanced photosynthesis and growth in fed plants. The poor pitcher

Table 5. *Parameters of leaf gas exchange and chlorophyll a fluorescence*

Parameter	*I*	*F*	*W*	*A*	*B*	*C*	*C0*
A_n (μmol m^{-2} s^{-1})	5.43 ± 0.67^{a}	5.61 ± 0.58^{a}	5.80 ± 0.35^{a}	5.12 ± 0.84^{ab}	3.50 ± 0.56^{bc}	2.05 ± 0.43^{c}	2.21 ± 0.20^{c}
g_s (mol m^{-2} s^{-1})	0.110 ± 0.008^{a}	0.102 ± 0.015^{a}	0.102 ± 0.009^{a}	0.096 ± 0.017^{a}	0.052 ± 0.011^{b}	0.053 ± 0.009^{b}	0.047 ± 0.009^{b}
g_m (mol m^{-2} s^{-1})	0.055 ± 0.015^{a}	0.054 ± 0.011^{a}	0.062 ± 0.007^{a}	0.045 ± 0.011^{ab}	0.037 ± 0.008^{abc}	0.012 ± 0.004^{c}	0.024 ± 0.002^{bc}
g_{tot} (mol m^{-2} s^{-1})	0.030 ± 0.006^{a}	0.028 ± 0.006^{ab}	0.031 ± 0.002^{a}	0.025 ± 0.005^{ab}	0.016 ± 0.003^{bc}	0.009 ± 0.002^{c}	0.012 ± 0.001^{c}
R_{dark} (μmol m^{-2} s^{-1})	0.620 ± 0.056^{a}	0.193 ± 0.029^{c}	0.509 ± 0.085^{ab}	0.595 ± 0.188^{a}	0.573 ± 0.104^{ab}	0.288 ± 0.065^{bc}	0.509 ± 0.078^{ab}
$V_{cmax}^{\ in\ vivo}$ (μmol m^{-2} s^{-1})	24.8 ± 1.6^{c}	26.3 ± 0.8^{c}	30.0 ± 1.0^{ab}	31.4 ± 1.8^{a}	26.7 ± 1.1^{bc}	17.7 ± 0.3^{d}	10.6 ± 0.4^{e}
J_{max} (μmol m^{-2} s^{-1})	61.0 ± 4.6^{c}	62.8 ± 1.5^{bc}	69.2 ± 2.4^{ab}	72.7 ± 3.9^{a}	62.1 ± 1.8^{bc}	37.8 ± 2.1^{d}	29.6 ± 0.8^{e}
F_v/F_m	0.787 ± 0.005^{abc}	0.799 ± 0.005^{a}	0.759 ± 0.013^{bc}	0.791 ± 0.006^{ab}	0.791 ± 0.004^{ab}	0.758 ± 0.018^{c}	0.725 ± 0.014^{d}
J (μmol m^{-2} s^{-1})	59.2 ± 4.7^{b}	61.3 ± 2.1^{ab}	68.4 ± 2.1^{a}	70.2 ± 4.4^{a}	58.9 ± 2.3^{b}	36.7 ± 1.9^{c}	25.6 ± 0.8^{d}
Φ_{CO2} (mol CO_2 mol^{-1} quanta)	0.016 ± 0.001^{b}	0.022 ± 0.001^{a}	0.022 ± 0.002^{a}	0.012 ± 0.003^{bc}	0.008 ± 0.002^{c}	0.007 ± 0.002^{c}	0.008 ± 0.001^{c}

Parameters shown are: net CO_2 assimilation rate (A_n), stomatal conductance (g_s), leaf mesophyll conductance to CO_2 (g_m), leaf total conductance to CO_2 (g_{tot}), mitochondrial respiration rate in darkness (R_{dark}), maximum velocity of Rubisco carboxylation ($V_{cmax}^{\ in\ vivo}$) and electron transfer (J_{max}), maximum quantum yield of PSII (F_v/F_m), electron transport rate (J) and apparent quantum yield of CO_2 fixation (Φ_{CO2}).

Values are means ± s.e. Different letters show significant differences in each parameter ($P < 0.05$, post-hoc Duncan's test, $n = 4$).

Treatments are *C0* = initial group, *C* = control, *B* = beetles, *A* = ants, *W* = wasps, *F* = flies, *I* = root fertilized with inorganic solution.

digestion of Ca is in accordance with the literature on the genus *Drosera* (Adamec, 2002; Pavlovič *et al.*, 2014), where the high Ca content in digested insects was attributed to a high concentration of Ca found in the mucilage secretion of *Drosera* and digestive fluid of *Nepenthes* (Nemček *et al.*, 1966; Rost and Schauer, 1977).

Leaf mineral composition altered the leaf biochemistry enhancing the photochemical and carboxylation potential of Nepenthes × ventrata

Chlorophyll concentration increased proportionally to leaf N after insect feeding or application of inorganic solution (Fig. 2A), as found in previous studies (Farnsworth and Ellison, 2008; Pavlovič *et al.*, 2009, 2011, 2014; He and Zain, 2012). Higher chlorophyll concentration occurred in line with an improved light absorption capacity performance and photochemistry denoted by an increase in F_v/F_m, Φ_{PSII} and Φ_{CO2} (Table 5; Supplementary data Figs S2 and S3). The higher relative abundance of pigment–protein complexes of PSI and PSII, components of the oxygen-evolving complex (PsbO, PsbP and PsbQ), electron transport (Cyt*f*) and ATPase in insect-fed and root-fertilized treatments (Fig. 3) provides the molecular explanation for the general improvement of the photochemical capacity after treatment application. Regarding COX and AOX, treatment *B* presented the lowest content of AOX, which was compensated by the highest content of COX (Fig. 3). This treatment also had the lowest stimulation of photosynthesis (Table 5), suggesting that plants fed with beetles may retain sugar and energy by maintaining a high COX:AOX ratio for effective ATP synthesis. Nevertheless, more information on AOX activity is needed to confirm specific trends in the regulation of the alternative respiratory pathway in *Nepenthes* × *ventrata*.

The results also demonstrated a causal relationship between the increase in leaf N concentration and the concentration of leaf TSP and Rubisco catalytic sites (Fig. 2). In particular, the increased concentration of Rubisco catalytic sites was promoted by the higher protein abundance of the Rubisco small subunit (RbcS) in all nutrient-treated plants, while differences in the relative abundance of the Rubisco large subunit (RbcL) between the control treatments and the insect-fed and root-fertilized plants were much less obvious (Fig. 3). This result indicates, for the first time in carnivorous plants, that N availability regulates the concentration of Rubisco via changes in the level of RbcS abundance, while RbcL abundance is rather constant irrespective of the nutrient status. Although the important role of RcbS in the regulation of Rubisco concentration was underlined by Suzuki and Makino (2012), the levels of RbcS and RbcL were maintained proportionally, as found by Imai *et al.* (2005) under different inorganic N applications in rice. However, there are also results indicating that RbcS can dramatically decline while the level of RbcL is sustained or decreased only very slightly (Bate *et al.*, 1991; Suzuki and Makino, 2013). Less invariable levels of RbcL in *Nepenthes* may be an adaptation for rapid recovery of the Rubisco concentration when new inputs of N are available.

In contrast to the concentration of Rubisco, the activation of Rubisco catalytic sites only increased in treatments *I* and *F* compared with control plants (Table 3). Taking this together with the fact that V_{cmax} increased in fed plants (Table 5), the conclusion is that the improvement in the carboxylation capacity of plants under root-fertilized and insect-fed treatments was achieved by an increase in the concentration of Rubisco (Fig. 4).

The present study is the first reporting a full dissection of Rubisco kinetic properties of a carnivorous plant. Rubisco from *Nepenthes* × *ventrata* displayed lower K_c, K_o and $k_{cat}^{\ c}$ compared with Rubisco from *Triticum aestivum* (Table 4). This is in contradiction to the proposed Rubisco selection towards higher $k_{cat}^{\ c}$ in carnivorous plants (Galmés *et al.*, 2014; Pavlovič and Saganová, 2015). Notably, the Rubisco CO_2/O_2 specificity ($S_{c/o}$) of *Nepenthes* × *ventrata* is one of the lowest values ever reported for a C_3 species (Galmés *et al.*, 2016; Hermida-Carrera *et al.*, 2016; Orr *et al.*, 2016), probably due to a lower $k_{cat}^{\ c}/K_c$ ratio and a relatively higher affinity for O_2 as compared with other species. In any case, the presence of particular kinetic characteristics of Rubisco from carnivorous plants, such as those described here for *Nepenthes* × *ventrata*, needs to be confirmed by means of screening a large number of carnivorous

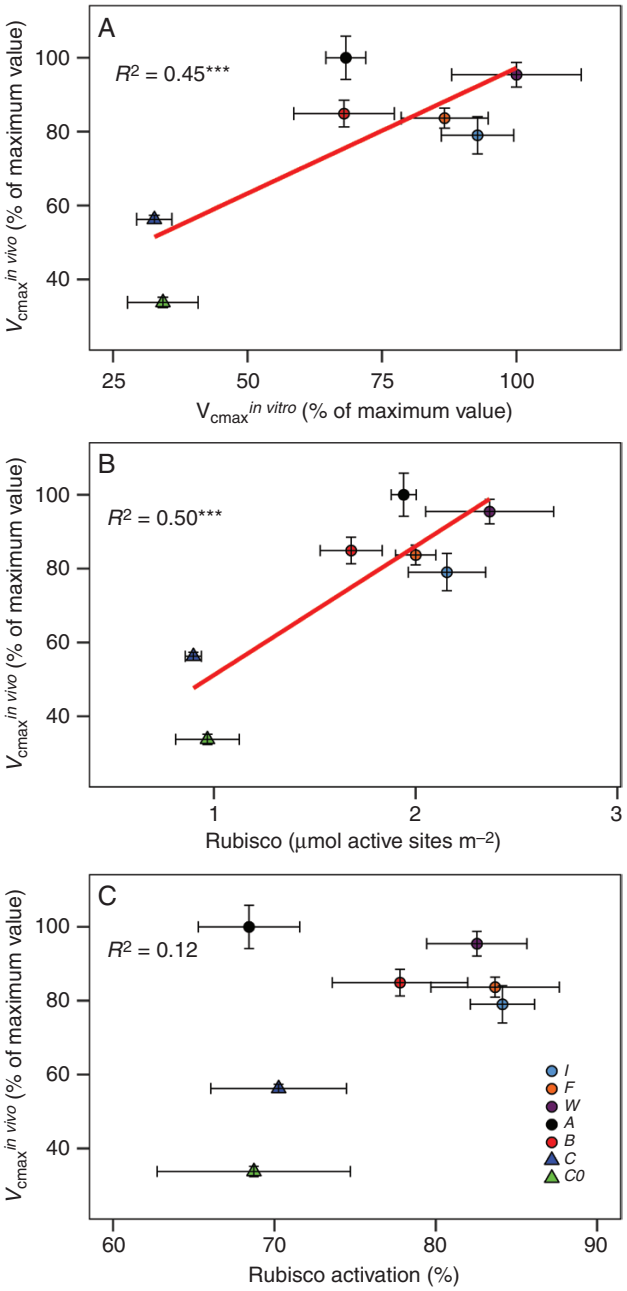

FIG. 4. Correlation between (A) $V_{cmax}^{in\ vitro}$ and $V_{cmax}^{in\ vivo}$; (B) correlation between Rubisco active sites concentration and $V_{cmax}^{in\ vivo}$; (C) correlation between Rubisco activation and $V_{cmax}^{in\ vivo}$. Points are means ± s.e. of different treatments: *C0* = initial group, *C* = control, *B* = beetles, *A* = ants, *W* = wasps, *F* = flies, *I* = root fertilized with inorganic solution. R^2 is Pearson's regression coefficient, and asterisks show the significance of test correlation (*$P < 0.05$; **$P < 0.01$; ***$P < 0.001$).

species in order to ascertain specific trends in the evolution of Rubisco in this group of plants.

Biochemical and mesophyll limitations were the major constraints for carbon assimilation in Nepenthes × ventrata

As a consequence of the improvement in the photochemical and carboxylation potential, the net CO_2 assimilation rate (A_n) was increased in plants of insect-fed and root-fertilized treatments, except for plants fed with beetles (Table 5). The increase in A_n was also accompanied by a general increase in the CO_2 diffusive capacity by means of higher g_s and g_m, in agreement with previous studies conducted in *Nepenthes* species (Pavlovič *et al.*, 2009, 2010; He and Zain, 2012).

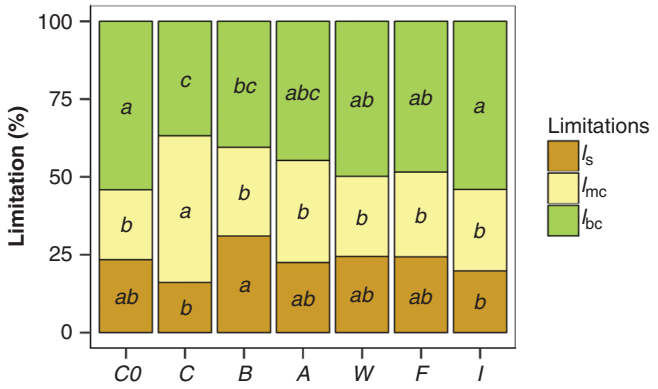

FIG. 5. Quantitative limitation analysis of photosynthetic CO_2 assimilation. Stomatal (l_s), leaf mesophyll (l_{mc}) and biochemical (l_{bc}) limitations are represented. Values are means, and different letters show significant differences in each limitation parameter among treatments ($P < 0.05$, post-hoc Duncan's test, $n = 4$). Treatments are *C0* = initial group, *C* = control, *B* = beetles, *A* = ants, *W* = wasps, *F* = flies, *I* = root fertilized with inorganic solution.

Previous studies suggested that carnivorous species present a compact leaf mesophyll which may restrict CO_2 diffusion towards Rubisco catalytic sites (Hodick and Sievers, 1989; Juniper *et al.*, 1989; Méndez and Karlsson, 1999; Pavlovič *et al.*, 2007), although the quantitative assessment of the limitation exerted by restricted g_m on the photosynthetic CO_2 assimilation rate was lacking. Here, we provide the first evidence that low g_m is the main photosynthetic limitation in nutrient-deprived carnivorous plants (Table 5; Fig. 5). The observed increase in g_m in plants with insect or root mineral nutrient application occurred along with a trend for an increase in the area of palisade occupied by air spaces (f_{ias}) (Table 5). Furthermore, we observed a negative correlation between the g_m and the T_{cw} of palisade cells (Fig. 6). This relationship has been well documented among angiosperms (Carriquí *et al.*, 2015), and suggests that thick cell walls and limited air spaces in the leaf mesophyll determine the low CO_2 diffusion in *Nepenthes* × *ventrata*.

In plants fed with insects or fertilized with inorganic solution, the general increase in g_m and decrease in l_{mc} were paralleled by a relative increase in biochemical limitation (l_{bc}) of photosynthesis (Fig. 5), despite the higher biochemical capacity (e.g. V_{cmax}) found in these treatments (Table 5). These results indicate that the alleviation of g_m after nutrient application resulted in a proportionally higher limitation by biochemistry than by leaf mesophyll conductance.

The most prominent difference in the effect of root fertilization vs. insect-feeding nutrition was observed in the biomass allocation to vegetative organs

In general, the plant growth rate increased with both insect feeding and root fertilization treatments (Supplementary data Table S4), probably due to a higher availability of

TABLE 6. *Leaf anatomical parameters*

Treatment	*I*	*F*	*W*	*A*	*B*	*C*	*C0*
LMA (g m^{-2})	86.6 ± 6.3^{a}	70.3 ± 8.2^{a}	81.0 ± 4.8^{a}	75.8 ± 3.3^{a}	69.4 ± 4.8^{a}	72.7 ± 3.6^{a}	78.3 ± 1.4^{a}
Mesophyll f_{ias} (%)	22.5 ± 1.6^{a}	20.7 ± 0.5^{a}	20.6 ± 2.0^{a}	24.6 ± 1.5^{a}	23.3 ± 1.5^{a}	16.3 ± 1.9^{a}	21.0 ± 1.6^{a}
Spongy f_{ias} (%)	31.9 ± 3.1^{a}	30.5 ± 1.4^{a}	32.8 ± 4.2^{a}	38.4 ± 1.4^{a}	35.0 ± 2.8a	24.5 ± 3.0^{a}	32.5 ± 2.0^{a}
Palisade f_{ias} (%)	7.49 ± 0.25^{ab}	9.16 ± 1.24^{a}	6.57 ± 0.64^{bc}	5.77 ± 0.72^{bc}	7.87 ± 1.10^{ab}	4.67 ± 0.61^{c}	5.80 ± 0.35^{bc}
Mesophyll T_{cw} (µm)	0.290 ± 0.030^{a}	0.283 ± 0.032^{a}	0.306 ± 0.015^{a}	0.356 ± 0.020^{a}	0.350 ± 0.037^{a}	0.365 ± 0.031^{a}	0.321 ± 0.021^{a}
Spongy T_{cw} (µm)	0.329 ± 0.039^{a}	0.326 ± 0.054^{a}	0.354 ± 0.028^{a}	0.415 ± 0.027^{a}	0.390 ± 0.053^{a}	0.409 ± 0.059^{a}	0.350 ± 0.027^{a}
Palisade T_{cw} (µm)	0.236 ± 0.019^{ab}	0.225 ± 0.027^{b}	0.250 ± 0.010^{ab}	0.260 ± 0.022^{ab}	0.294 ± 0.040^{ab}	0.302 ± 0.009^{a}	0.276 ± 0.012^{ab}

Leaf mass area (LMA), percentage of the area occupied by air spaces [f_{ias} (%)] of mesophyll, spongy and palisade cells, and cell wall thickness (T_{cw}) of mesophyll, spongy and palisade cells (see Supplementary data Fig. S4).

Values are means ± s.e. Different letters show significant differences in each parameter ($P < 0.05$, post-hoc Duncan's test, $n = 4$).

Treatments are *C0* = initial group, *C* = control, *B* = beetles, *A* = ants, *W* = wasps, *F* = flies, *I* = root fertilized with inorganic solution.

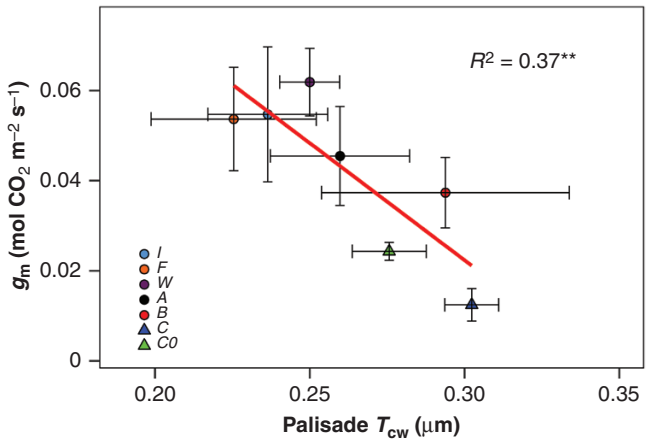

FIG. 6. Correlation between mesophyll conductance (g_m) and cell wall thickness of palisade cells (Palisade T_{cw}). Points are means ± s.e. of different treatments: *C0* = initial group, *C* = control, *B* = beetles, *A* = ants, *W* = wasps, *F* = flies, *I* = root fertilized with inorganic solution. R^2 is Pearson's regression coefficient, and asterisks show the significance of test correlation (*$P < 0.05$; **$P < 0.01$; ***$P < 0.001$).

photoassimilates promoted by enhanced photosynthesis. In relative terms, plants under treatment *I* allocated much more of the new biomass to leaves than plants fed with insects, where the main fraction for biomass allocation was in their pitchers (Supplementary data Fig. S5). Pavlovič *et al.* (2009, 2010) also found that N administration via inorganic solution did not favour pitcher formation in *N. talangensis*, in contrast to insect feeding. *Sarracenia purpurea* also decreased allocation to the carnivorous structure (pitcher tube diameter vs. keel size) in response to an inorganic N addition into the traps (Ellison and Gotelli, 2002), but not in response to insect feeding (Wakefield *et al.*, 2005). Thus, carnivory is probably controlled by both quantity and form of nutrient input.

Conclusion

This study resolved a 35-year-old hypothesis proposed by Givnish *et al.* (1984) that carnivorous plants should increase photosynthetic assimilation via enhanced Rubisco synthesis from prey-derived N. In addition to this, N from prey is also used for synthesis of chlorophylls and their binding proteins, thus enhancing the efficiency of photochemistry. The present work also demonstrates that the principal photosynthetic limitation in nutrient-stressed *Nepenthes* × *ventrata* is the mesophyll CO_2 diffusion. This was relieved after the insect-fed and root-fertilized treatment application due to an increase in mesophyll conductance, resulting in a higher biochemistry limitation in treated plants. Differences between insect-fed and root-fertilized treatments were minor and restricted to plant biomass allocation, where treatment with soil inorganic nutrient application invests more biomass into the assimilation leaves than insect-fed treatments which maintained pitcher growth.

SUPPLEMENTARY DATA

Supplementary data are available online at https://academic.oup.com/aob and consist of the following. Figure S1: photograph of plants before and after treatments. Figure S2: means of A_n–C_c curves for each treatment and means of Φ_{PSII}–PPFD curves for each treatment. Figure S3: correlation between maximum quantum yield of PSII and total chlorophyll content and correlation between electron transport rate and total chlorophyll content. Figure S4: microscopic optic photograph of leaves of treatment *C* and treatment *I*. Figure S5: proportion of biomass increase of each plant fraction. Table S1: mineral concentration of leaves of *Nepenthes* × *ventrata*. Table S2: amount of each element in total leaf tissue of *Nepenthes* × *ventrata*. Table S3: amount of element administered to plants in each insect-fed treatment and percentage removed by digestion. Table S4: different growth parameters. Method S1: additional methodological details on Rubisco kinetic measurements. Method S2: additional methodological details on western blot analysis.

FUNDING

This work was financially supported by the Spanish Ministry of Science and Innovation project AGL2013-42364-R awarded to J.G. from the Spanish Ministry of Economy and Competitiveness (MINECO) and the ERDF (FEDER).

ACKNOWLEDGEMENTS

We thank Son Suau farmland for their agreement for us to capture insects on their properties. We are grateful to Dr Cyril Douthe for Li-Cor technical assistance, to Mateu Fullana and Marc Carriquí for their support in plant sampling and anatomical measurements,

and Biel Martorell for his technical help on the IRMS. We would like to thank Trinidad Garcia and Concepción Iñiguez for their technical help and organization of the radioisotope installation at the Serveis Científico-Tècnics of UIB while running these experiments. The authors declare that the research was conducted in the absence of any commercial or financial relationships that could be construed as a potential conflict of interest.

LITERATURE CITED

Adamec L. 2002. Leaf absorption of mineral nutrients in carnivorous plants stimulates root nutrient uptake. *New Phytologist* **155**: 89–100.

Adamec L. 2008. The influence of prey capture on photosynthetic rate in two aquatic carnivorous plant species. *Aquatic Botany* **89**: 66–70.

Bate NJ, Rothstein SJ, Thompson JE. 1991. Expression of chloroplast photosynthesis genes during leaf senescence. *Journal of Experimental Botany* **42**: 801–811.

Bernacchi CJ, Singsaas EL, Pimentel C, Portis a RJ, Long SP. 2001. Improved temperature response functions for models of Rubisco-limited photosynthesis. *Plant, Cell & Environment* **24**: 253–260.

Bradford MM. 1976. A rapid and sensitive method for the quantitation of microgram quantities of protein utilizing the principle of protein–dye binding. *Analytical Biochemistry* **72**: 248–254.

von Caemmerer S. 2000. Biochemical models of leaf photosynthesis. *Techniques in Plant Sciences* **53**: 1689–1699.

Carriquí M, Cabrera HM, Conesa MÀ, *et al.* 2015. Diffusional limitations explain the lower photosynthetic capacity of ferns as compared with angiosperms in a common garden study. *Plant, Cell & Environment* **38**: 448–460.

Chin L, Chung AYC, Clarke C. 2014. Interspecific variation in prey capture behavior by co-occurring *Nepenthes* pitcher plants. Evidence for resource partitioning or sampling-scheme artifacts? *Plant Signaling & Behavior* **9**: e27930.

Dixon KW, Pate JS, Bailey WJ. 1980. Nitrogen nutrition of the tuberous sundew *Drosera erythrorhiza* lindl. with special reference to catch of arthropod fauna by its glandular leaves. *Australian Journal of Botany* **28**: 283–297.

Ellison AM. 2006. Nutrient limitation and stoichiometry of carnivorous plants. *Plant Biology (Stuttgart, Germany)* **8**: 740–747.

Ellison AM, Adamec L, eds. 2018. *Carnivorous plants: physiology, ecology, and evolution*. Oxford: Oxford University Press.

Ellison AM, Gotelli NJ. 2002. Nitrogen availability alters the expression of carnivory in the northern pitcher plant, *Sarracenia purpurea*. *Proceedings of the National Academy of Sciences, USA* **99**: 4409–4412.

Ellison AM, Gotelli NJ. 2009. Energetics and the evolution of carnivorous plants—Darwin's 'most wonderful plants in the world'. *Journal of Experimental Botany* **60**: 19–42.

Farnsworth EJ, Ellison AM. 2008. Prey availability directly affects physiology, growth, nutrient allocation and scaling relationships among leaf traits in 10 carnivorous plant species. *Journal of Ecology* **96**: 213–221.

Farquhar GD, von Caemmerer S, Berry JA. 1980. A biochemical model of photosynthetic CO_2 assimilation in leaves of C_3 species. *Planta* **149**: 78–90.

Flexas J, Díaz-Espejo A, Berry JA, *et al.* 2007. Analysis of leakage in IRGA's leaf chambers of open gas exchange systems: quantification and its effects in photosynthesis parameterization. *Journal of Experimental Botany* **58**: 1533–1543.

Galmés J, Medrano Hip 'lito, Flexas J. 2007. Photosynthetic limitations in response to water stress and recovery in Mediterranean plants with different growth forms. *New Phytologist* **175**: 81–93.

Galmés J, Kapralov MV, Andralojc PJ, *et al.* 2014. Expanding knowledge of the Rubisco kinetics variability in plant species: environmental and evolutionary trends. *Plant, Cell & Environment* **37**: 1989–2001.

Galmés J, Hermida-Carrera C, Laanisto L, Niinemets Ü. 2016. A compendium of temperature responses of Rubisco kinetic traits: variability among and within photosynthetic groups and impacts on photosynthesis modeling. *Journal of Experimental Botany* **67**: 5067–5091.

Galmés J, Molins A, Flexas J, Conesa MÀ. 2017. Coordination between leaf CO_2 diffusion and Rubisco properties allows maximizing photosynthetic efficiency in *Limonium* species. *Plant, Cell & Environment* **40**: 2081–2094.

Gao P, Loeffler TS, Honsel A, *et al.* 2015. Integration of trap- and root-derived nitrogen nutrition of carnivorous *Dionaea muscipula*. *New Phytologist* **205**: 1320–1329.

Givnish TJ, Burkhardt EL, Happel RE, Weintraub JD. 1984. Carnivory in the bromeliad *Brocchinia reducta*, with a cost/benefit model for the general restriction of carnivorous plants to sunny, moist, nutrient-poor habitats. *The American Naturalist* **124**: 479–497.

Harley PC, Loreto F, Di Marco G, Sharkey TD. 1992. Theoretical considerations when estimating the mesophyll conductance to CO_2 flux by analysis of the response of photosynthesis to CO_2. *Plant Physiology* **98**: 1429–1436.

He J, Zain A. 2012. Photosynthesis and nitrogen metabolism of *Nepenthes alata* in response to inorganic and organic prey N in the greenhouse. *ISRN Botany* **2012**: 263270, doi: 10.5402/2012/263270.

Hermida-Carrera C, Kapralov MV, Galmés J. 2016. Rubisco catalytic properties and temperature response in crops. *Plant Physiology* **171**: 2549–2561.

Hodick D, Sievers A. 1989. On the mechanism of trap closure of Venus flytrap (*Dionaea muscipula* Ellis). *Planta* **179**: 32–42.

Imai K, Suzuki Y, Makino A, Mae T. 2005. Effects of nitrogen nutrition on the relationships between the levels of rbcS and rbcL mRNAs and the amount of ribulose 1,5-bisphosphate carboxylase/oxygenase synthesized in the eighth leaves of rice from emergence through senescence. *Plant, Cell & Environment* **28**: 1589–1600.

Juniper B, Robins R, Joel D. 1989. *The carnivorous plants*. London: Academic Press.

Klunder HC, Wolkers-Rooijackers J, Korpela JM, Nout MJR. 2012. Microbiological aspects of processing and storage of edible insects. *Food Control* **26**: 628–631.

Kouřimská L, Adámková A. 2016. Nutritional and sensory quality of edible insects. *NFS Journal* **4**: 22–26.

Kruse J, Gao P, Honsel A, *et al.* 2014. Strategy of nitrogen acquisition and utilization by carnivorous *Dionaea muscipula*. *Oecologia* **174**: 839–851.

Kubien DS, Brown CM, Kane HJ. 2011. Quantifying the amount and activity of Rubisco in leaves. *Methods in Molecular Biology* **684**: 349–362.

Lichtenthaler H, Wellburn A. 1983. Determinations of total carotenoids and chlorophylls *b* of leaf extracts in different solvents. *Biochemical Society Transactions* **11**: 591–592.

Martins SCV, Galmés J, Molins A, Damatta FM. 2013. Improving the estimation of mesophyll conductance to CO_2: on the role of electron transport rate correction and respiration. *Journal of Experimental Botany* **64**: 3285–3298.

Méndez M, Karlsson PS. 1999. Costs and benefits of carnivory in plants: insights from the photosynthetic performance of four carnivorous plants in a subartic enviroment. *Oikos* **86**: 105–112.

Moran JA, Merbach MA, Livingston NJ, Clarke CM, Booth WE. 2001. Termite prey specialization in the pitcher plant *Nepenthes albomarginata* – evidence from stable isotope analysis. *Annals of Botany* **88**: 307–311.

Nemček O, Sigler K, Kleinzeller A. 1966. Ion transport in the pitcher of *Nepenthes henryana*. *Biochimica et Biophysica Acta* **126**: 73–80.

Orr DJ, Alcântara A, Kapralov MV, Andralojc PJ, Carmo-Silva E, Parry MA. 2016. Surveying Rubisco diversity and temperature response to improve crop photosynthetic efficiency. *Plant Physiology* **172**: 707–717.

Pavlovič A, Saganová M. 2015. A novel insight into the cost–benefit model for the evolution of botanical carnivory. *Annals of Botany* **115**: 1075–1092.

Pavlovič A, Masarovičová E, Hudák J. 2007. Carnivorous syndrome in Asian pitcher plants of the genus *Nepenthes*. *Annals of Botany* **100**: 527–536.

Pavlovič A, Singerová L, Demko V, Hudák J. 2009. Feeding enhances photosynthetic efficiency in the carnivorous pitcher plant *Nepenthes talangensis*. *Annals of Botany* **104**: 307–314.

Pavlovič A, Singerová L, Demko V, Šantrůček J, Hudák J. 2010. Root nutrient uptake enhances photosynthetic assimilation in prey-deprived carnivorous pitcher plant *Nepenthes talangensis*. *Photosynthetica* **48**: 227–233.

Pavlovič A, Slováková Ľ, Šantrůček J. 2011. Nutritional benefit from leaf litter utilization in the pitcher plant *Nepenthes ampullaria*. *Plant, Cell & Environment* **34**: 1865–1873.

Pavlovič A, Krausko M, Libiaková M, Adamec L. 2014. Feeding on prey increases photosynthetic efficiency in the carnivorous sundew *Drosera capensis*. *Annals of Botany* **113**: 69–78.

Pavlovič A, Krausko M, Adamec L. 2016. A carnivorous sundew plant prefers protein over chitin as a source of nitrogen from its traps. *Plant Physiology and Biochemistry* **104**: 11–16.

Perdomo JA, Carmo-Silva E, Hermida-Carrera C, Flexas J, Galmés J. 2016. Acclimation of biochemical and diffusive components of photosynthesis in rice, wheat, and maize to heat and water deficit: implications for modeling photosynthesis. *Frontiers in Plant Science* **7**: 1–16.

Ramos-Elorduy J, Moreno JMP, Prado EE, Perez MA, Otero JL, De Guevara OL. 1997. Nutritional value of edible insects from the state of Oaxaca, Mexico. *Journal of Food Composition and Analysis* **10**: 142–157.

Rost K, Schauer R. 1977. Physical and chemical properties of the mucin secreted by *Drosera capensis*. *Phytochemistry* **16**: 1365–1368.

Schulze E-, Gebauer G, Schulze W, Pate JS. 1991. The utilization of nitrogen from insect capture by different growth forms of *Drosera* from Southwest Australia. *Oecologia* **87**: 240–246.

Schulze W, Schulze ED, Pate JS, Gillison AN. 1997. The nitrogen supply from soils and insects during growth of the pitcher plants *Nepenthes mirabilis*, *Cephalotus follicularis* and *Darlingtonia californica*. *Oecologia* **112**: 464–471.

Shi X, Sun H, Pan H, *et al.* 2016. Growth and efficiency of nutrient removal by *Salix jiangsuensis* J172 for phytoremediation of urban wastewater. *Environmental Science and Pollution Research International* **23**: 2715–2723.

Sui H, Clarke C. 2015. Prey capture patterns in *Nepenthes* species and natural hybrids – are the pitchers of hybrids as effective at trapping prey as those of their parents? *Carnivorous Plant Newsletter* **44**: 62–79.

Suzuki Y, Makino A. 2012. Availability of Rubisco small subunit up-regulates the transcript levels of large subunit for stoichiometric assembly of its holoenzyme in rice. *Plant Physiology* **160**: 533–540.

Suzuki Y, Makino A. 2013. Translational downregulation of RBCL is operative in the coordinated expression of Rubisco genes in senescent leaves in rice. *Journal of Experimental Botany* **64**: 1145–1152.

Wakefield AE, Gotelli NJ, Wittman SE, Ellison AM. 2005. Prey addition alters nutrient stoichiometry of the carnivorous plant *Sarracenia purpurea*. *Ecology* **86**: 1737–1743.